Peer-reviewed version available at *Sensors* **2020**, *20*, 4560; doi:10.3390/s20164560

Type of the Paper (Article)

Non-Invasive PPG-Based System for Continuous Heart Rate Monitoring of Incubated Avian Embryo

Ali Youssef [1], Daniel Berckmans[1] and Tomas Norton[1],*

[1] Faculty of Bioscience Engineering, Katholieke Universiteit Leuven (KU LEUVEN), Kasteelpark Arenberg 30, 3001 Heverlee/ Leuven, Belgium;

* Correspondence: tomas.norton@kuleuven.be ; Tel.: +32 16377531

List of abbreviations:

AB: Amplification circuit board
ACG: Acoustocardiogram
APG: Acceleration Plethysmogram
BCG: Ballistocardiogram
CAM: Chorioallantoic Membrane
CWT: Continuous Wavelet Transform
DFT: Discrete Fourier Transform
DOG: Derivative of Gaussian
ECG: Electrocardiogram
ECW: Embryonic Cardiac Wave
ED: Embryonic Day
FFT: Fast Fourier Transform
HPF: High-Pass Filter
HR: Heart Rate
ICG: Impedance Cardiogram
iPPG: image Photoplethysmographic
LB: LED's Control Circuit Board
LED: Light-Emitting Diode
LPF: Low-Pass Filter
LVR: Linear Voltage Regulator
PGA: Programmable Gain Amplifier
PPG: Photoplethysmography
SNR: Signal-to-Noise Ratio
TIA: Transimpedance Amplifier
WT: Wavelet Transform

Abstract:

The chicken embryo is a widely used experimental animal-model in many studies such as developmental biology and to study the physiological responses and adaptation to altered environments as well as for cancer and neurobiology research. Embryonic heart rate is an important physiological variable useful as an index reflecting the embryo's natural activity and is considered one of the most difficult parameters to measure. An acceptable measurement technique of embryonic heart rate should provide a reliable cardiac signal quality while maintaining adequate gas exchange through the eggshell along the incubation and embryonic developmental period. In this paper, we presented a detailed design and methodology for a non-invasive PPG-based

prototype (Egg-PPG) for real-time and continuous monitoring of embryonic heart rate during incubation. An automatic embryonic cardiac wave detection algorithm, based on normalised spectral entropy, is described. The developed algorithm successfully estimated the embryonic heart rate with 98.7% accuracy. We believe that the developed overall system presented in this paper is showing a promising solution for non-invasion, real-time monitoring of embryonic cardiac signal, which can be used in both experimental studies (e.g., developmental embryology and cardiovascular research) and in industrial incubation applications.

Keywords: Embryonic Heart Rate; Photoplethysmography (PPG); Continuous Wavelet Transform (CWT); Spectral Entropy

1. Introduction

The chicken embryo is not only an important product in the worldwide demand for chicken meat but is also a widely used experimental animal model in developmental biology research. It is often used for studying physiological responses and adaptation to altered environments as well as for neurobiology research [1]–[3]. The chick chorioallantoic membrane (CAM) assays have been widely used to study angiogenesis, tumour cell invasion metastasis. The CAM model has many advantages, such as (a) the highly vascularised nature of the CAM greatly promotes the efficiency of tumour cell grafting; (b) high reproducibility and (c) simplicity and cost effectiveness [4]. Chicken eggs can be incubated to any stage of interest, simplifying experimental design. Within two to three days of laying, chick embryos gastrulate, neurulate, and fold into three-dimensional (3D) animals with beating hearts, somites, and complex nervous systems [5]. Moreover, chicken embryos are semi-transparent, making viewing of internal tissues and organs possible under the microscope. Many parameters of interest can be monitored during the development of the embryo. Heart rate (HR) is an important physiological variable useful as an index reflecting the embryo's natural activity and traditionally has been one of the most difficult parameters to measure [6]

The heart is the first functioning organ during the developmental stage of the avian embryo [7]. The maturing tissues and organs require a higher oxygen consumption during later stages of development. This can only be met by an increasing oxygen delivery when blood flow finally takes place. The heart rate of a chicken embryo is therefore an important autonomic controlled index of the cardiovascular system [8]. The heart rate (HR) of chicken embryos during incubation and before hatching can be a very useful physiological parameter for evaluating the regulation mechanisms of the cardiovascular system and the thermoregulatory development. Photoplethysmography (PPG) is a measurement of heart beat rate based on changes in the flow rate of the blood flow. Unlike Electrocardiogram (ECG), which measures the heart rate by placing electrodes on the patient's chest measuring electrical potential, PPG is a low cost, simple, non-invasive optical measurement based upon reflection of light and used in biomedical field to detect blood volume changes in the microvascular bed of tissue through red and infrared lights [9].

In the literature, cardiogenic signals of avian embryos are detectable by various sensors noninvasively, semi-invasively or invasively while maintaining adequate gas exchange through the eggshell [10], [11].

As cited by Bellville [12] and Romanoff [13], the early research works of Bogue [14] in 1932, showed that the heart rate of chicken embryos could in those days only be studied using an electrocardiogram (ECG). In this technique, at least three electrodes have to be inserted into the tissues surrounding the embryo.

Later, Bamelis et al. [11] used an ECG measuring technique in which the electrodes were positioned between the shell and the outer membrane. However, due to the exposed holes in the eggshell exchange of gaseous environment (i.e. water vapour, oxygen and carbon dioxide) of the embryo and thus influence the embryo's physiology [11]. Moreover, long-term recording of heart-

rate in this way is risky, due to the increased possibility of bacterial infections passing through the exposed holes.

The same concerns are also presented in the case of the Impedance Cardiogram (ICG), developed by Tazawa and Whittow [15] and the pulse-oximetry technique first presented by Lewin et al., [8].

To overcome these concerns, different researchers have developed various techniques to measure the heart-rate. Several invasive and less invasive techniques were tested and demonstrated to measure chicken embryo longer term heart rate and heart rate variability [16]–[18].

The Ballistocardiogram (BCG) is based on slight movements or vibrations of the eggshell, caused by contraction of the embryonic heart, which can be detected by piezoelectric sensors [19] or optically via laser interference [3]. The Acoustocardiogram (ACG) uses the effect of the pulsatile air movement across the eggshell, detected by microphone [20] or differential pressure transducer [21]. In their work [20], Rahn et al. developed a technique, which involved placing an egg in a tightly sealed vessel containing a condenser microphone. Akiyama et al. [10] measured Instantaneous Heart Rate (IHR) in chicken embryos using an Acoustocardiogram (ACG) from day 12 till hatching. They found that IHR comprised transient bradycardia and tachycardia, which first developed on day 14 and 16 in most embryos, respectively.

Youssef et al. [22] introduced a novel way for real-time, semi-invasive measurement of embryonic heart rate based on image photoplethysmographic (iPPG) techniques by making a little window (1 cm^2) in the eggshell. Although the developed technique by Youssef et al. [22] provided a continuous and real-time measurements of the developing embryo during incubation, yet it is an invasive technique, which needs careful handling and otherwise a contamination can take place.

Although many efforts and research has been done on continuous long term monitoring of HR in chicken embryos, so far no practical and affordable technique, implementable in commercial incubators, is available. In the present work, we present a full description of a prototype of a non-invasive PPG-based system, including hardware and real-time algorithm, for continuous long-term heart rate monitoring of the developing chicken embryo during incubation.

2. Photoplethysmographic (PPG)-based embryonic heart rate extraction

In general, the photoplethysmographic (known most commonly as PPG) system is consisting of a light source (usually light-emitting diode) and a photodiode to detect the light. When a light-emitting diode (LED) emits light, it passes through living body (tissue) and can be absorbed by the surrounding substances like arterial blood, venous blood, bone and skin [23]. The absorption of this light can either be constant (bone and skin) or alternating (arterial blood). The alternating occurrence in arterial blood is attributable to the greater blood flow rate or volume per unit of time at systolic phase, while being less during diastolic phase. Depending on the relative position of the photodiode to the light source, two different modes of operation are existing, namely, transmittance and reflective modes. In the reflectance mode, the light emitter is placed next to the detector, which measures the backscattered or reflected light from the tissue (body). On the other hand, in the transmittance mode, the photodiode is placed in the opposite position of the light emitter in such way that the photodiode only detect the transmitted light through the body.

Many studies have previously indicated that the green light (495–570 nm) is showing a higher absorptivity for oxygenated blood than other spectrums (e.g., [23], [24]). In general, short wavelengths (i.e., green and blue) are known to have a lower *penetration depth* (δ) than longer wavelengths (i.e., red and infrared) [25], [26]. This is the depth when light intensity decreases with 37% of the intensity on the incident surface [24]. Therefore, short wavelengths are more common in detecting superficial blood flow while deeper tissue movements have less impact.

The penetration depth is described as [26]:

$$\delta = \frac{1}{\sqrt{3\mu_a(\lambda).\left(\mu_a(\lambda) + \mu_s(\lambda)\right)}}$$

where δ is the penetration depth (mm), μ_a and μ_s are the absorption and scattering coefficients (cm). The penetration depth depends mainly on the *extinction coefficient* of the tissue or the material through which the light is passing. This extinction coefficient is defined as the sum of both absorption and scatter coefficients (i.e., $(\mu_a(\lambda) + \mu_s(\lambda))$). Light travels longer through tissue when they have low absorptive and scatter properties [24]. Wavelengths such as red and infrared have low coefficients in most biological tissue, explaining why they are used in the transmittance mode.

2.1. Hardware design and prototype (Egg-PPG)

The main components of the designed and developed Egg-PPG prototype are presented as a block diagram in Figure 1. The Egg-PPG prototype consists of the two main components, namely, the light source system and the photodiode system.

2.1.1. Light source system

The light source system comprises of the following:

a) The light emitting diodes (LED's)

Three infrared LED's (from Würth Elektronik), L_0, L_1 and L_2 (Figure 1) with emitting peak wavelength (λ_{peak}) of 945 nm and maximum radiant intensity of 300 mW·Sr^{-1} (at ~1 A) are used as the light source in the Egg-PPG.

b) The LED's control board

Due to the continuous changes in the internal physical and optical properties of the incubated egg, as results of the embryonic development, the Egg-PPG is designed in such way to adapt the light intensity of the three LEDs to insure high quality PPG signal along the embryonic developmental stages. Thus, LED's control circuit board (LB) is developed to control the light intensity of the LEDs via a linear voltage regulator (LVR). The developed LED control board is provided with an external input terminal (0-5 DC-Volt), which allows the user to externally control the LEDs current and consequently regulating the LEDs intensity between 0 and 300 mW·Sr^{-1}.

2.1.2. Photodiode system

The Photodiode system comprises of the following:

a) Photodiode light sensor

One photodiode (SFH 2201 OSRAM), P (Figure 1), characterised with a wavelength of maximum sensitivity of 950 nm and radiant sensitivity area of 8.12 mm2 is used in the Egg-PPG.

b) Amplification board

When reflected/transmitted light is partly absorbed by the photodiode, a very small current I_P, with an order of Nano-amperes (photodiode maximum current = 74nA), is produced. This photodiode maximum current (I_{Pmax}= 74nA) is equivalent to the direct current (DC) signal of the received light. While the embryonic cardiac waves appear as a small alternative current (AC) signal that is superimposed on the baseline DC signal. Hence, an amplification circuit board (AB) is developed to amplify and condition the photodiode signal (Figure 1). The output of the amplification board is a PPG voltage signal (V_{out} = -5V to +5V), which can be readout using a suitable data acquisition interface. The developed AB consists of the following main components:

- *Transimpedance amplifier*

The transimpedance amplifier (TIA) converts the very small current I_P, produced by the photodiode, into a readable voltage. The TIA has a gain stage equal to the feedback resistor value $R_{feedback}$, where the voltage output of the TIA is given by $V_{TIA} = I_P \times R_{feedback}$.

- *Analog filters*

The amplification circuit board contains a low-pass filter (LPF) with a cut-off frequency of 16Hz to filter out the high frequency TIA noises, which are originated mainly from the input voltage noise (noise gain), the input current noise and the thermal noises (resistor). Additionally, a high-pass filter (HPF), with a cut-off frequency of 23mHz, eliminates the DC-offset originated from the constant LED light.

- *Programmable gain amplifier*

A programmable gain amplifier (PGA) gives an external control of the TIA gain with 10 gain levels from -10 to -100 dB (with 10 dB incremental steps), which can be controlled using an external digital I/O interface. The PGA gives the possibility and flexibility to adapt the received PPG signal to maximize the signal-to-noise ratio (SNR).

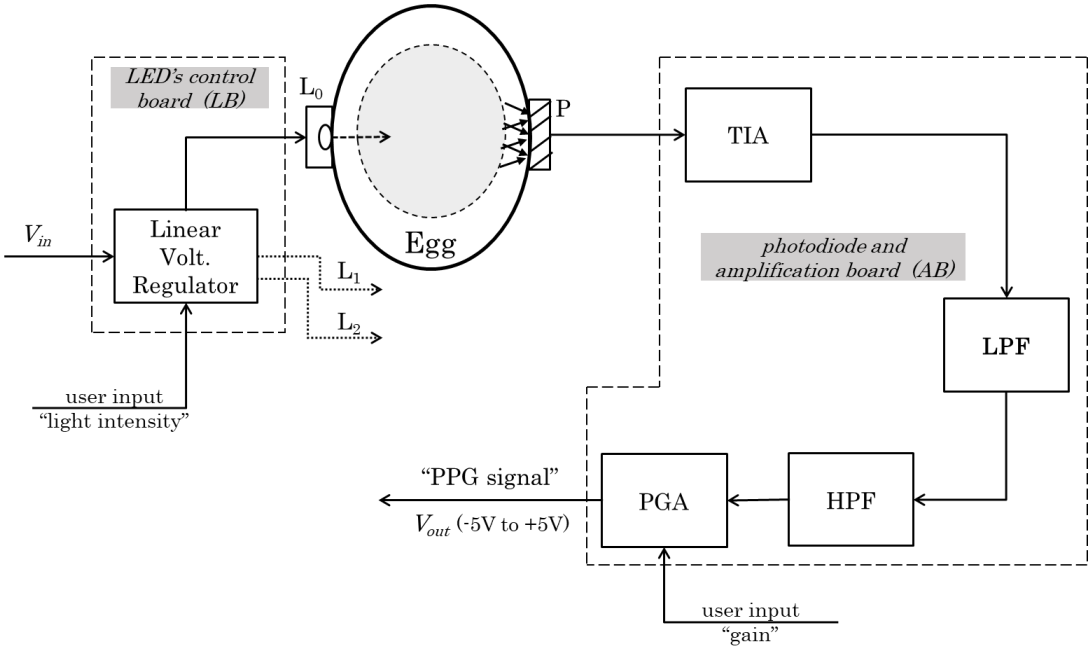

Figure 1. Hardware main components of the developed prototype (Egg-PPG) shows the LED's control circuit board (**LB**) for the infrared LED's (**L0**, **L1** and **L2**), photodiode (**P**) and the photodiode and amplification circuit board (**AB**) includes a transimpedance amplifier (**TIA**), low-pass filter (**LPF**), high-pass filter (**HPF**) and programmable gain amplifier (**PGA**).

Preprints (www.preprints.org) | NOT PEER-REVIEWED | Posted: 26 July 2020 doi:10.20944/preprints202007.0651.v1

Peer-reviewed version available at Sensors 2020, 20, 4560; doi:10.3390/s20164560

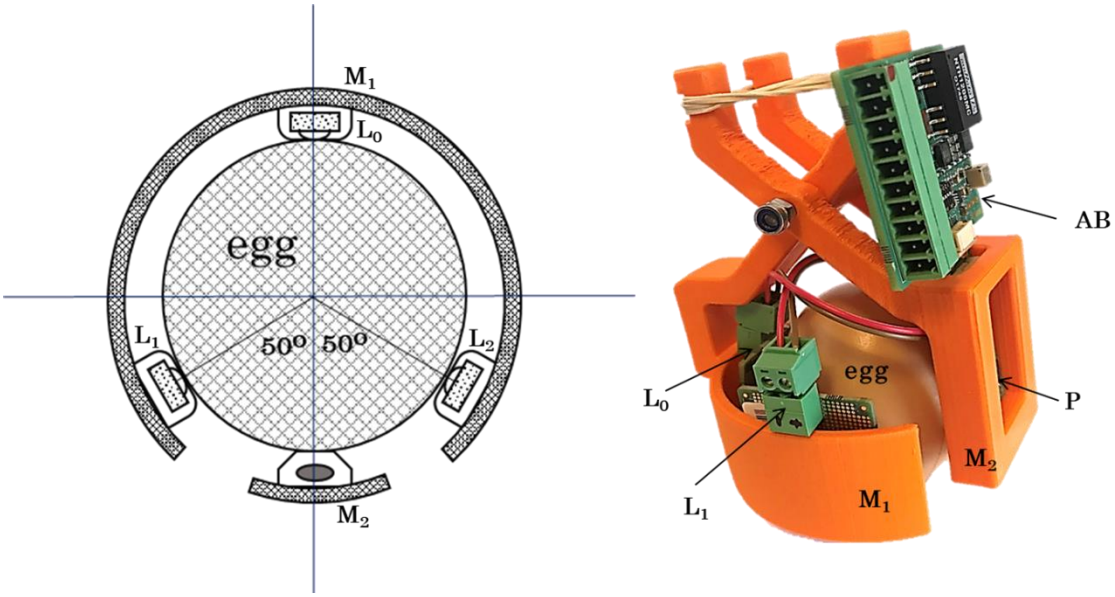

Figure 2. (left graph) a top-view schematic representation of the developed Egg-PPG prototype shows the relative positions of the three infrared LEDs (**L0**, **L1** and **L2**), photodiode (**P**) and the two sections (**M1** and **M2**) of the Egg-PPG housing system (**HS**), (right graph) the corresponding photographic picture of the Egg-PPG prototype shows the photodiode and amplification circuit board (**AB**).

2.2. Embrypnic cardiac wave extraction algorithm and heart rate calculation

The main components of the continuous wavelet transform (CWT)-based embryonic cardiac wave (ECW) extraction algorithm are depicted in the following block diagram (Figure 3).

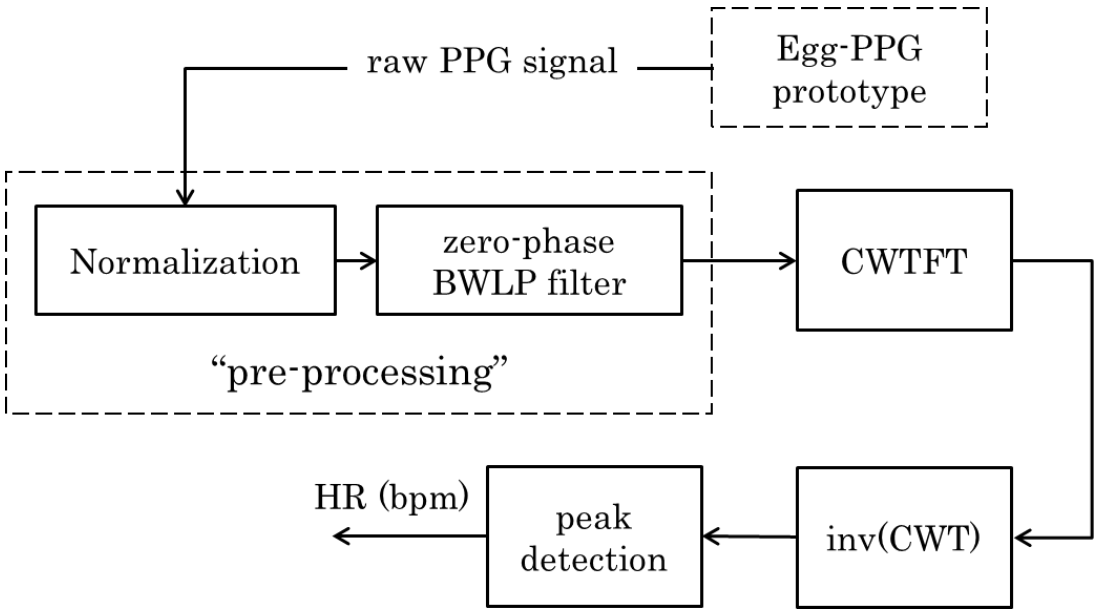

Figure 3. Block diagram showing the main signal processing steps to extract the embryonic heart rate using the Egg-PPG prototype. The block diagram includes the pre-processing, continuous wavelet transform Fourier transform (**CWTFT**) algorithm, invers continuous wavelet transform (**invCWT**) and peak detection algorithm blocks.

2.2.1. Pre-processing of PPG signals

Firstly, the PPG signals are normalized to zero mean and unit variance [27]. The normalized signals are filtered using a zero-phase 4th order Butterworth low pass (BWLP) filter with a cut-off frequency of 7 Hz. This cut-off frequency is chosen to contain, in the filter passband, the documented (e.g., [3], [10], [14], [28]) physiological heart rate range (160 – 300 bpm) of the chicken embryo during different developmental stages. The Butterworth filter is providing a maximally flat passband together with the zero-phase implementation are preserving the embryonic cardiac wave. The second derivative of the PPG signal, also called the acceleration plethysmogram (APG), shows more defined peaks than these of PPG signal and can are useful as a more accurate detection of heart rate [29]. In this paper, the APG is used, which shows more distinctive peaks than the PPG signal. Figure 4 is showing an example of the resulting APG signal after the pre-processing in comparison of the raw PPG signal obtained from an incubated fertile egg at embryonic day ED09. For more distinction of the cardiac wave peaks, the APG signal is squared that by squaring the positive values of the APG signal, while negative values are equated to zero (see an example in Figure 4).

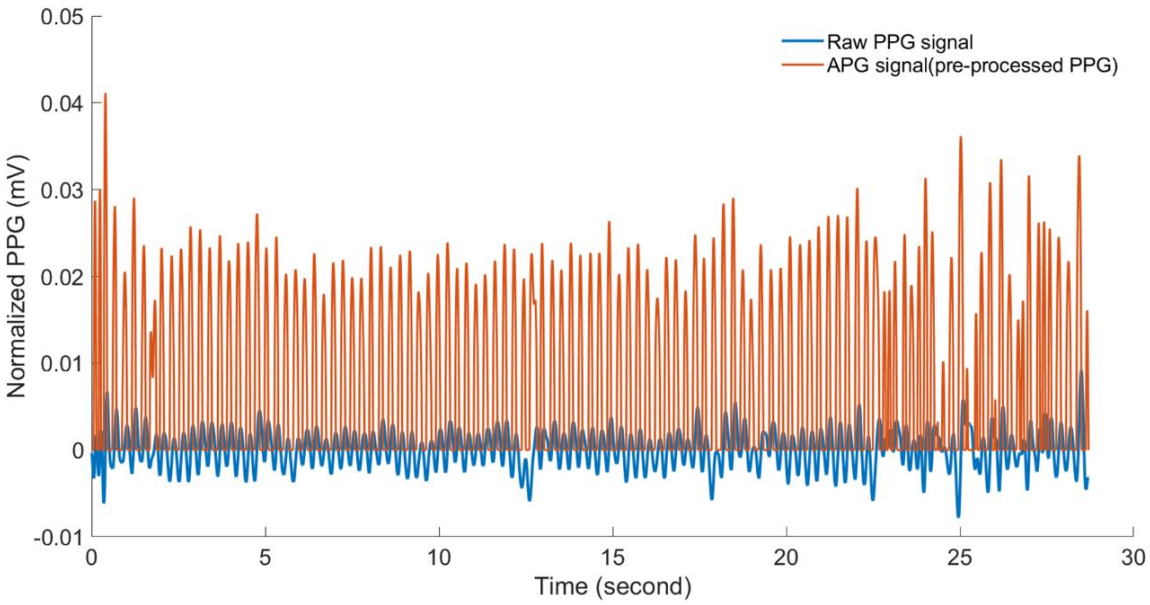

Figure 4. The acceleration plethysmogram (APG) signal (red line) resulting from the pre-processing in comparison to the raw PPG signal (blue line), obtained from an incubated fertile egg at embryonic day ED09.

2.2.2. Wavelet analysis and peak detection

Wavelet Transform (WT) is a spectral estimation technique by breaking a general function into an infinite series of wavelets [27]. In the biomedical engineering field, Wavelet transform (WT) is often preferred over Fast Fourier Transform (FFT) in signal processing because most of the physiological signals are non-stationary in nature, which makes WT a viable method. The wavelet transform can be used to analyse time series that contain nonstationary power at many different frequencies [30], [31]. Using WT, the signals in time domain are mapped into frequency domain to preserve both the time and frequency information.

- *Continuous Wavelet Transform method*

For the continuous wavelet transform (CWT) method of spectral decomposition, the kernel function is a wavelet that adapts to the frequency of interest. In general, a specific wavelet centred about a given frequency is computed from the mother wavelet by scaling it and shifting. In this manner, the length of the wavelet contains the same number of centre (also called peak) frequency cycles. For a scale parameter, $s > 0$ and a position parameter b, which defines a translation of the wavelet and indicates the time localization, the CWT can be given by [31]:

Peer-reviewed version available at Sensors 2020, 20, 4560; doi:10.3390/s20164560

$$C(s,b) = \int_{-\infty}^{+\infty} x(t) \frac{1}{\sqrt{s}} \psi^* \left(\frac{t-b}{s}\right) dt \quad (1)$$

The Wavelet analysis is performed by convoluting the signal under investigation (i.e., the VPG signal), $x(t)$, with a mother wavelet, $\psi(t)$. The $\psi^*(t)$ is the complex conjugate of the analyzing mother wavelet. While the term $\frac{1}{\sqrt{s}}$ is an energy normalized factor (the energy of the wavelet must be the same for different s values of the scale). By varying the scaling factor 's', the wavelet family can represent broadband spectra, wherein the spectrum of each wavelet in the family maintains a constant ratio between its peak frequency and the corresponding bandwidth [32]. In practice, the CWT is usually computed over discrete values of the 's' scale in the range of continuous values. To approximate the continuous wavelet transform, the equation (1) should be done N times for each scale, where N is the number of points in the discrete signal $f(t)$ [31]. The classic CWT transform is time consuming and it requires considerable computing power to be applied in real-time. More efficient algorithms have been developed for significant acceleration of CWT calculation [33]–[35].

In this paper, the CWT is calculated using fast Fourier transform (CWFT) [35] that is allowing to compute the N convolutions simultaneously, which is more suitable for real-time applications. The CWFT algorithm implements the following steps:

i. Obtain the discrete Fourier transform (DFT) of the analysed signal $x(n)$, includes N samples, using Fast Fourier Transform (FFT) as follows:

$$\hat{x}(k) = \sum_{n=0}^{N-1} x(n) e^{-i\frac{2\pi}{N}nk}, \; k = 0,1,2 \cdots N-1 \quad (2)$$

where k is an index of frequency.

ii. Obtain the DFT ($\hat{\psi}$) of the analysing wavelet (ψ) at the appropriate angular frequencies as follows:

$$\hat{\psi}(k) = \sum_{n=0}^{N-1} \psi(n) e^{-i\frac{2\pi}{N}nk}, \; k = 0,1,2 \cdots N-1 \quad (3)$$

iii. Scale the DFT of the analysing wavelet at different scales to ensure different scales are directly comparable.

In order to obtain the unit energy for each scale s, the wavelet function is normalized by the following formula:

$$\hat{\psi}(s\omega_k) = \sqrt{\frac{2\pi s}{\Delta t}} \hat{\psi}(s\omega_k), \quad (4)$$

where is the sampling period $\Delta t = 1/f_s$ with f_s is the sampling frequency and $\omega_k = \frac{2\pi k}{N\Delta t}$.

iv. Take the product of the signal DFT and the wavelet DFT over all the scales. Invert the DFT to obtain the CWT coefficients as follows:

$$W_s(b) = \frac{1}{N} \sqrt{\frac{2\pi s}{\Delta t}} \sum_{k=0}^{N-1} \hat{x}\left(\frac{2\pi}{N\Delta t}k\right) \hat{\psi}^*\left(s\frac{2\pi}{N\Delta t}k\right) e^{i\frac{2\pi}{N}kb}. \quad (5)$$

The Gaussian function is perfectly local in both time and frequency domains and is indefinitely derivable, a derivative of any order (m) of the Gaussian function may be a Wavelet Transform (WT). Typical cardiac pulse event in PPG signal consists of two modulus maxima with different signs of $W_s(s,b)$ (i.e., maxima and minima) [36]. Sahambi et al., [36], used a first order, odd function **错误!未找到引用源。**, to detect the QRS complex in the ECG signal.

Hence, a first order Derivative of Gaussian (DOG) wavelet is chosen for the presented work because, in general, the obtained scalograms (scales "s" vs. positions "b") using this wavelet showed clear frequency contents within the expected pulse rate ranges of the chicken embryo. The first order DOG wavelet is given as follows:

$$\psi(t) = -t\, exp^{\left(-\frac{t^2}{2}\right)}. \quad (6)$$

2.2.3. Power spectral entropy and embryonic cardiac wave recognition

The spectral entropy is used in different applications as a entropy-like index to identify the relative disorder in time dynamics of biological, ecological and physical systems [37]. Detection of the specific waveform of the embryonic cardiac wave (ECW) is a challenging process especially in the presence of non-stationary noise such as motion artefacts and during the early stages of embryonic development due to the relatively weak cardiac signal. To overcome such problem in applications such as speech recognition and end-point detection, the entropy-based algorithm is proposed by some investigators (e.g., [38], [39]). In the present work, we proposed an entropy-based algorithm for automatic ECW detection. The application of the entropy concept for ECW recognition is based on the assumption that the spectrum of the PPG signal is more organised (lower entropy) during the segments of cardiac events than during noise segments. The power spectral entropy (E_S) of the PPG signal is computed as follows [39]:

- The probability density function (PDF) of the spectrum of the PPG signal can be estimated by normalisation over all the frequency components:

$$P_i = \frac{S(f_i)}{\sum_{k=1}^{N_f} S(f_k)}, \qquad i = 1,2,\cdots N_f \quad (7)$$

where P_i is probability density for the $S(f_i)$, which is the spectral energy of the i^{th} frequency component f_i, obtained by fast Fourier transform (FFT) and N_f is the total number of frequency components in the FFT.

- Then, the spectral entropy (H_n) of PPG n^{th} segment is calculated as follows:

$$H_n = -\sum_{i=1}^{N_f} P_i \log_2 P_i. \quad (8)$$

Usually, the spectral entropy (H) is normalized by dividing equation (12) by $\log_2 N_f$, which represents the maximal spectral entropy of white noise, uniformly distributed in the frequency domain. In this paper, we propose different approach of normalization of the spectral entropy by dividing the PPG spectral entropy (H_n), equation (12), by the spectral entropy of a PPG segment obtained from infertile egg (H_∞). The normalized spectral entropy (E_S) is given as follows:

$$E_S = \frac{H_n}{H_\infty} = \frac{\sum_{i=1}^{N_f} P_i \log_2 P_i}{\sum_{i=1}^{N_f} P_{\infty i} \log_2 P_{\infty i}}, \quad (9)$$

where P_∞ is the probability density of the PPG segment obtained from interfile egg, which is representing, in our case, the maximal spectral entropy. Hence, it is expected that the normalized spectral entropy (E_S) of the PPG signal is equal or closer to unity in the absence of cardiac events.

2.2.4. Peak detection and heart rate calculation

In general, the heartbeat could be estimated by calculating the time between the peak intervals in the PPG signal. The peak is detected by calculating the local maxima of the decoupled cardiac pulse signal $X(n)$ within a predefined interval (window) I that by finding $n_o \in$ I fulfilling that:

$$X(n_o) \geq X(n), \forall n \in \text{I}$$

The algorithm then repeats the procedure of the tallest peak and iterate until it runs out of considerable peaks.

3. Experiment and measurements

3.1. Incubation and incbuated eggs

Thirty fertile eggs of broiler chickens (breed Ross 308 and flock age of 42 weeks) are incubated in an experimental incubator (a detailed description of the experimental incubator can be found in [40]) at 37.8°C, with relative air humidity of 60%, and automated turning every two hours. Another four infertile eggs are also placed as control (blank) test inside the incubator, during the whole incubation period.

3.2. Data acquesition and PPG measurments

A three dimensional (3D) printed plastic housing system (HS in Figure 2) is designed in a way to contain the three LEDs (L_0, L_1 and L_2) and the photodiode (P) around the egg (see Figure 2). The housing system (HS) consists of two sections, the largest one (M_1) is designed to hold the three LEDs around the egg with the possibility of place each LED around the vertical axis of the egg (see Figure 2). While the small section (M_2) is holding the photodiode (P) tightly around the egg.

The PPG signal obtained from the Egg-PPG prototype is a readout using the National Instrument® USB-6009 multifunction data-acquisition (DAQ) device as an interface between the Egg-PPG and the computer. A customized Matlab script is developed to interface/communicate with the Egg-PPG prototype through the National Instrument® USB-6009. Using the developed Matlab interface script, the PPG signal is acquired at 128Hz sampling rate and controls both light intensity of the three LEDs and amplification gain of the acquired PPG signal.

3.3. Detection of embryonic cardiac wave

During the first 24-30 hours of incubation, blood and vascular development initiate both in the form of extra-embryonic blood islands and intra-embryonic endothelial cell specification and differentiation [41], [42]. The first major blood vessels of the embryo, the paired dorsal aorta, have formed by 30-35 hours of development [42]–[44], and a beating heart is apparent by 38-42 hours of development [41], [45]. Thus, theoretically, the embryonic cardiac wave (ECW) is detectable between the second and third days of incubation. However, this is not the case in reality due to many practical difficulties related to the optical properties of the incubated eggs and the weak cardiac signal, especially in such early stage of development.

A successful detection of the ECW using the Egg-PPG prototype is depending on the choice of the suitable LED's intensity (I) and amplification gain (G). In this phase of investigation, starting from embryonic day ED03, a manual search for the ECW is performed by changing both LED's intensity and amplification gain. In total, combinations included 8 intensity (from 50 to 300mW.Sr^{-1} with 50mW.Sr^{-1} dB incremental steps) levels and 10 gains (from -10 to -100 dB with 10 dB incremental steps) to search for the ECW. For each combination a segment of 60 seconds of PPG measurement is recorded. After performing the pre-processing step, the spectral analysis is performed on the recorded PPG segment. Together with the visual inspection, the spectral analysis results are used to detect the presence of the ECW.

Once the ECW is detected, the PPG signal is acquired daily from three different fertile eggs. Each day the PPG measurement is done for 10 minutes per egg. The daily selection of the test eggs is done by random picking eggs from the incubation tray.

4. Results and discussion

4.1. Detection of embyonic cardiac wave and signal quality

The manual searching for the embryonic cardiac wave (ECW) showed that it is only possible to detect an ECW starting from embryonic day ED07 using the Egg-PPG prototype. The results showed that the ECW is detectable from ED07 until ED19 using light intensity range within I = 150 to 300 mW.Sr^{-1} and amplification gain range within G = -50 to -100dB.

The daily acquired PPG signals within ED07 until ED18, from all tested eggs, are divided into segments of 10 seconds each (i.e., 1280 data samples) to be processed individually. In total, 180 PPG segments are analysed per each embryonic day (ED) from ED7 until ED18. After the pre-processing

step (see section 2.3.1), the continuous wavelet transform of each segment is computed using the CWTFT algorithm. The tricky step of embryonic cardiac wave (ECW) decoupling using CWT is the selection of the most suitable set of scales (s).

The suitable set of scales (s) should contain most of the energy of the ECW. We found that the energy of the cardiogenic pulse signals, in all acquired PPG segments, is dominated five scales between 0.05 and 0.10. Figure 5 shows an example scalogram showing the distribution of the calculated CWT coefficients (and energy) over the different scales (s), based on PPG signal obtained from fertile eggs at embryonic ED09. The resulting scalogram (example Figure 5) showed that most of the energy (calculated from CWT coefficients) is dominating the selected scale range (005-0.10).

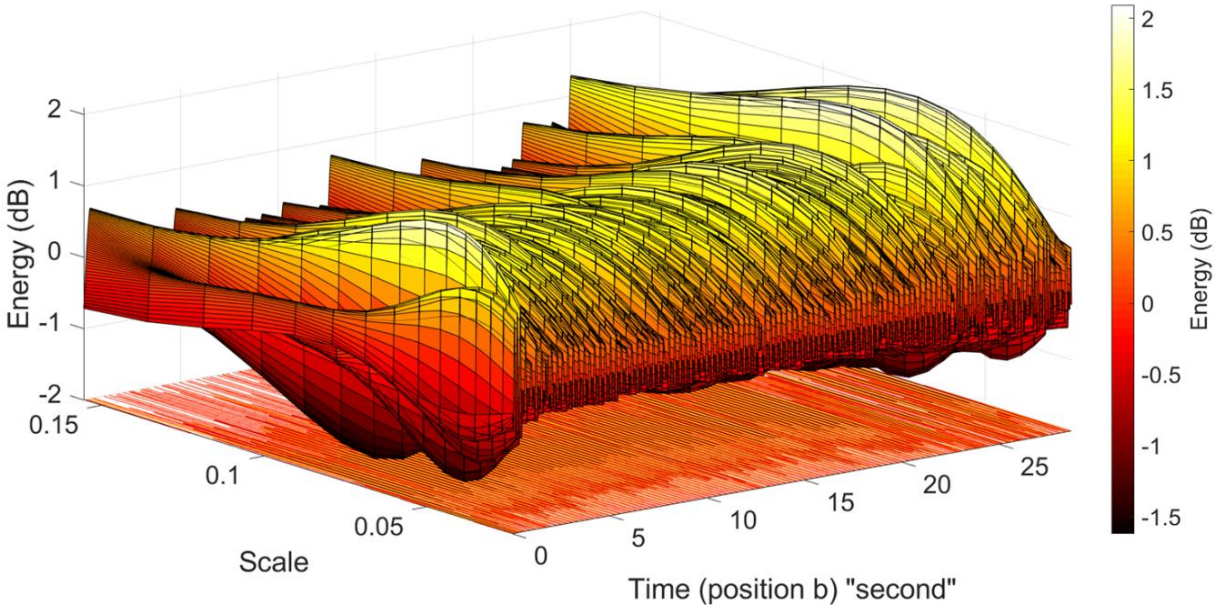

Figure 5. As the scalogram shows the distribution of the calculated energy using the CWTFT algorithm for the PPG segment, obtained from incubated fertile egg at embryonic day ED09, most of the energy is dominating scale range from 0.05 to 0.10.

4.2. Embryonic cadiac wave extraction and heart rate calculation

The developed CWT-based ECW extraction algorithm is used to extract and reconstruct the ECW from each PPG segment, obtained from the tested fertile eggs, during the incubation period between ED07 until ED18. The instantaneous embryonic heart rate (bpm) based on the inter peaks interval is calculated using the peak detection algorithm. The results showed that the reconstructed ECW in all cases is not affected by the dicrotic notch, which is a secondary upstroke in the descending part of a pulse tracing corresponding to the transient increase in aortic pressure upon closure of the aortic valve [46] that can lead to false reading of the peaks (Figure 6).

In Figure 7, the daily averages and standard deviations (represented as error bars) of the estimated embryonic heart rate are shown as calculated from the acquired daily PPG segments between embryonic days ED07 and ED18. The resulting estimations of the daily embryonic heart rate, using the developed Egg-PPG and ECW estimation algorithm, are comparable to the documented (e.g., [3], [10], [14], [22]) heart rates using different techniques (e.g., ECG, ICG, Pulse-Oximetry, and semi-invasive iPPG-based system).

Although, the estimated embryonic heart rate is within the expected and documented daily embryonic heart rate, the developed Egg-PPG system together with the ECW extraction algorithm are yet to be validated. A validation technique based on visual inspection (labelling) of the ECW and manual counting of the peaks is used as a ground-truth heart rate (reference). In total, 30 PPG-segments are visually labelled and HRs are manually calculated and then compared to the corresponding estimated HR using the developed ECW extraction algorithm. Results showed that

Preprints (www.preprints.org) | NOT PEER-REVIEWED | Posted: 26 July 2020 doi:10.20944/preprints202007.0651.v1

Peer-reviewed version available at Sensors 2020, 20, 4560; doi:10.3390/s20164560

the average estimated HRs using the developed ECW extraction algorithm are in agreement with the manually calculated HRs with an accuracy of 98.7%. An ECG-based heart rate measurement technique, as reported by Aubert et al. [1], is attempted to be used as a gold-standard for this work. However, we did not succeed to obtain a reliable measurement of the embryonic ECG.

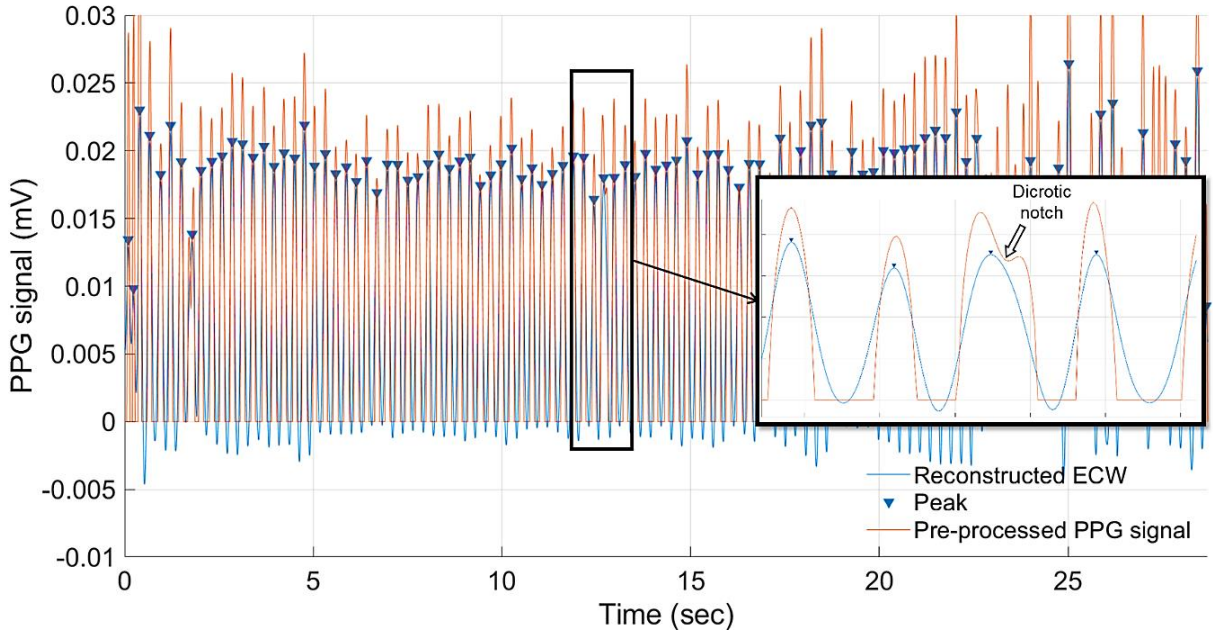

Figure 6. Detected cardiac peaks based on the reconstructed embryonic cardiac wave (ECW) in comparison to a pre-processed PPG segment obtained from incubated fertile egg at embryonic day ED09. The zoomed graph shows that the developed ECW extraction algorithm is not susceptible to false readings of the dicrotic notch.

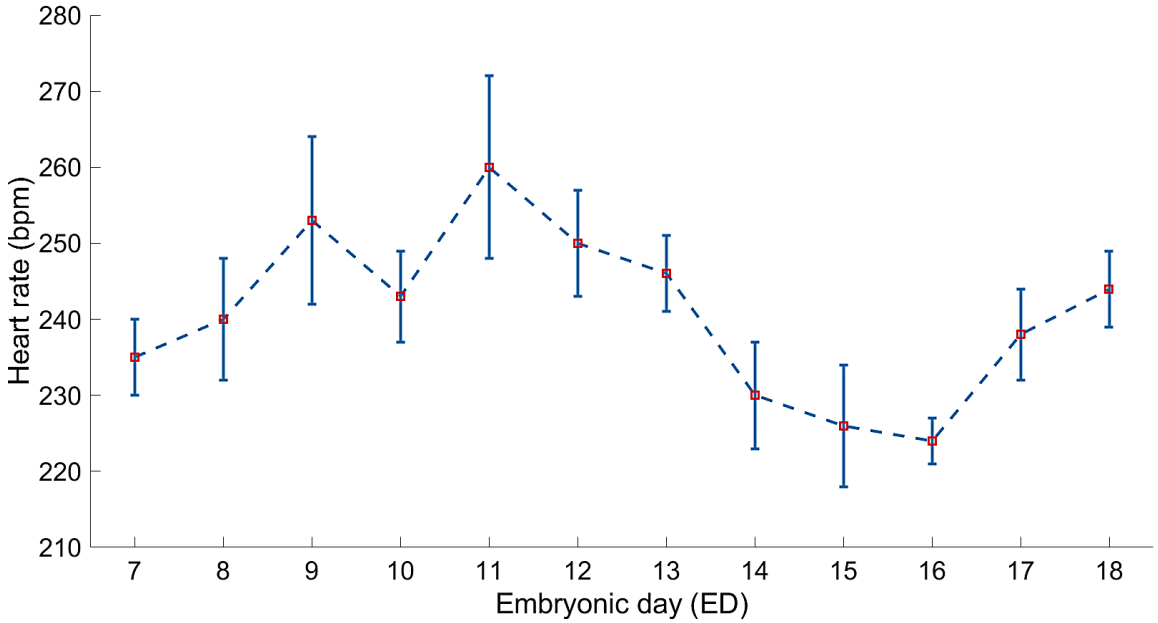

Figure 7. Average ±standard deviation (error bars) estimated embryonic daily heart rate based on the acquired PPG segments using the developed Egg-PPG prototype and embryonic cardiac wave extraction algorithm.

4.3. Real-time heart rate monitoring algorithm

Preprints (www.preprints.org) | NOT PEER-REVIEWED | Posted: 26 July 2020 doi:10.20944/preprints202007.0651.v1

Peer-reviewed version available at Sensors 2020, 20, 4560; doi:10.3390/s20164560

A main challenge to realize a robust real-time embryonic heart rate monitoring system is developing an automatic ECW detection algorithm. As mentioned earlier, the reliability of the acquired PPG signal is depending on the selected LED's intensity I and amplification gain. G. Therefore, to find the most suitable I and G, at which the ECW is detectable, a search over all possible combinations of both variables is needed. Additionally, a reliable feature variable is needed as an indicator for ECW. In this paper, the normalised spectral entropy (E_S) is used as a feature variable to detect the ECW. The assumption here is that the PPG epoch with ECW contains more information (low spectral entropy) in comparison with the PPG epoch with no ECW as in infertile egg. To test this approach, the normalised spectral entropy of 25 PPG segments acquired from infertile eggs (i.e., contained no ECW) and other 25 segments acquired from fertile eggs with labelled ECW. The E_S values of the PPG segments that contain no ECW are found always around 1±0.04. While the PPG segments with labelled ECW epochs showed lower levels of E_S (0.65±0.1). Figure 8 shows that a PPG segment (upper graph) consists of two epochs of PPG signal with no ECW sandwiching another with labelled ECW and the corresponding normalised spectral entropy (lower graph). As shown in Figure 8, the plot of E_S differentiates the epoch with the ECW from that without.

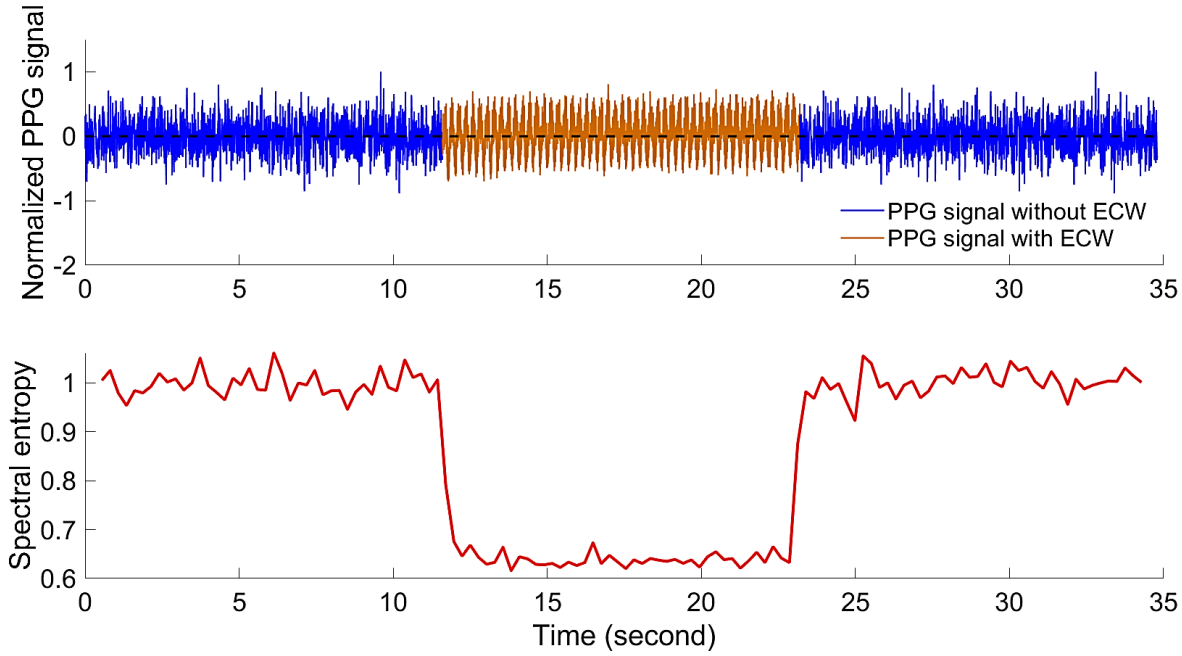

Figure 8. Normalized PPG signal with and without the embryonic cardiac wave (ECW) and the corresponding normalised spectral entropy (E_S).

Based on the 95% percentile of all the ECW epochs, a spectral entropy (E_S) threshold confidence interval between 0.56 (lower threshold) and 0.69 (upper threshold) where 95% of the ECW exist is defined.

An automatic ECW detection algorithm is proposed based on normalised spectral entropy as shown in the flow chart depicted in Figure 9 and the following pseudo-code :

```
PPG_signal(Gi,Ij)
INPUT: Gi ϵ{-50,-60,-70,-80,-90,-100}dB;and Ij ϵ{150,200,250,300} mW.Sr-1
LOOP initiation: i = 0 and j = 0; i ϵ{0,1,2,3,4,5}; j ϵ{0,1,2,3}
FOR:  Gi and Ij
    DO: record 15 seconds of PPG_signal(Gi,Ij)
    DO: calculate ES
IF: lower_threshold ≤ ES ≤ upper_threshold
    DO: PPG_signal(Gi,Ij) contains ECW
    DO: continue recording
```

```
ELSE:
    DO: continue LOOP
END
```

The proposed algorithm is based on examining a PPG segment of 15 seconds at each combination of amplification gain (G) and LED's intensity (I), which makes the maximum time of testing all combinations to be 6 minutes and yet sufficient to detect the ECW.

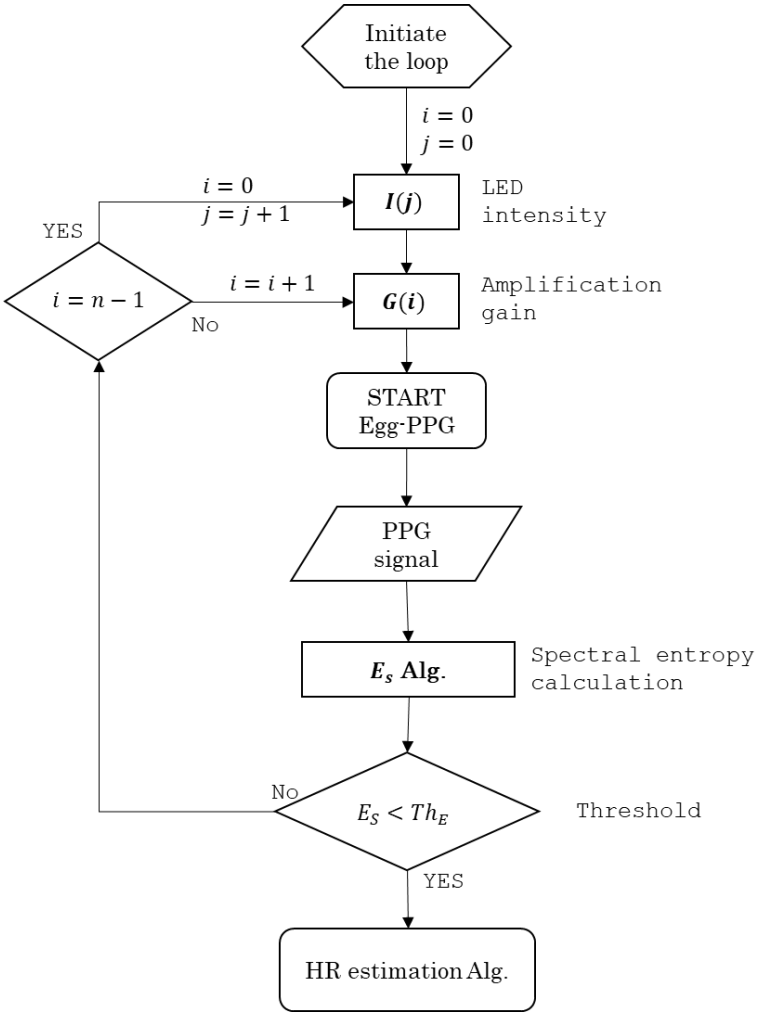

Figure 9. Flow chart shows the main steps of the developed cardiac signal detection algorithm based on spectral entropy (E_S).

The developed ECW detection algorithm is tested offline against 10 recorded PPG segments that include cardiac (ECW) and non-cardiac epochs. The results showed that the algorithm successfully detects the ECW epochs with more than 98% accuracy. Figure 10 shows an example of a PPG segment obtained from a fertile egg at embryonic day ED09 that contains two manually labelled epochs of ECW and other non-cardiac ones. As shown in the figure, during the ECW epochs the calculated spectral entropy values are within the defined thresholds.

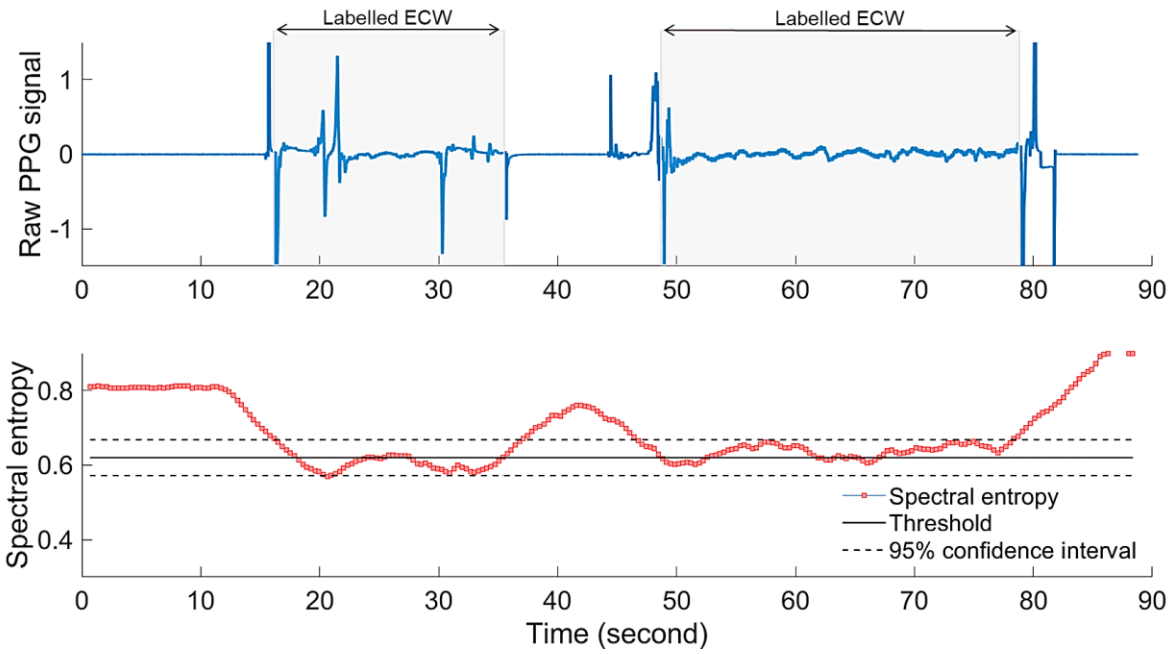

Figure 10. Raw PPG signal (upper graph) showing signal regions including cardiac waves (shaded regions) and regions with no cardiac waves, additionally the corresponding calculated spectral entropy, E_S, (lower graph) of the raw PPG signal shows the defined E_S thresholds for cardiac signal.

5. Conclusions

In this paper, we presented a detailed design and methodology for a non-invasive PPG-based prototype (Egg-PPG) for real-time and continuous monitoring of embryonic heart rate during incubation. A developed automatic embryonic cardiac wave (ECW) detection algorithm based on normalised spectral entropy is described. The ECW detection algorithm is successfully detecting the ECW epochs in the test PPG segments with 98% accuracy. The resulting heart rate of the developed embryonic heart rate estimation algorithm is compared to manually labelled and calculated heart rates. The results showed that the algorithm successfully estimated the embryonic heart rate with 98.7% accuracy. The developed prototype is showing a promising solution for non-invasion, real-time and continuous monitoring of embryonic heart rate during incubation. However, further validation work is yet recommended in future research work.

Author Contributions: "Conceptualization, A.Y.; methodology, A.Y.; software, A.Y.; validation, A.Y.; formal analysis, A.Y.; investigation, A.Y.; resources, D.B. and T.N.; data curation, A.Y.; writing—original draft preparation, A.Y.; writing—review and editing, A.Y. D.B. and T.N.; visualization, A.Y.; supervision, D.B. and T.N.; project administration, T.N.; funding acquisition, A.Y., D.B. and T.N. All authors have read and agreed to the published version of the manuscript.", please turn to the CRediT taxonomy for the term explanation. Authorship must be limited to those who have contributed substantially to the work reported.

Acknowledgments: The authors gratefully thank to the technical and financial support of Petrsime NV. (Belgium) and the support of Petersime R&D team, namely, Luc Gabrial, Eduardo Romanini, Rudy Verhelst, Pascal Garain and Paul Degraeve. Additionally, all authors are showing a kind appreciation to Dekimo NV. team, namely, Eddy Vanhoecke, Jo Gabriel, Laurent Cattoir and Steven Vancoppenolle, for the technical support to realise the Egg-PPG prototype.

Conflicts of Interest: "The authors declare no conflict of interest."

References

[1] A. E. Aubert *et al.*, "Heart rate and heart rate variability in chicken embryos at the end of incubation.," *Exp. Physiol.*, vol. 89, no. 2, pp. 199–208, Mar. 2004.

[2] H. Tazawa, "Effect of O2 and CO2 in N2, He, and SF6 on chick embryo blood pressure and heart rate.," *J. Appl. Physiol.*, vol. 51, no. 4, pp. 1017–22, Oct. 1981.

[3] H. Tazawa, T. Hiraguchi, T. Asakura, H. Fujii, and G. C. Whittow, "Noncontact measurements of avian embryo heart rate by means of the laser speckle: comparison with contact measurements," *Med. Biol. Eng. Comput.*, vol. 27, no. 6, pp. 580–586, Nov. 1989.

[4] N. A. Lokman, A. S. F. Elder, C. Ricciardelli, and M. K. Oehler, "Chick Chorioallantoic Membrane (CAM) Assay as an In Vivo Model to Study the Effect of Newly Identified Molecules on Ovarian Cancer Invasion and Metastasis.," *Int. J. Mol. Sci.*, vol. 13, no. 8, pp. 9959–70, Jan. 2012, doi: 10.3390/ijms13089959.

[5] R. S. Tuan and C. W. Lo, *Developmental Biology Protocols*, vol. 135. New Jersey: Humana Press, 1999.

[6] T. H, A. A, M. K, G. E, and P. JT, "Embryonic heart rate measurements during artificial incubation of emu eggs," *Br. Poult. Sci.*, vol. 41, no. 1, 2000.

[7] J. G. Wittig and A. Münsterberg, "The Early Stages of Heart Development: Insights from Chicken Embryos.," *J. Cardiovasc. Dev. Dis.*, vol. 3, no. 2, Apr. 2016.

[8] R. Lewin, M. Dörner, and H. Tönhardt, "Pulse oximetry: a new way of determining the heart rate in chicken embryos," *Pflügers Arch. Eur. J. Physiol.*, vol. 434, no. 5, pp. 639–641, Aug. 1997.

[9] J. Allen, "Photoplethysmography and its application in clinical physiological measurement," *Physiol. Meas.*, vol. 28, no. 3, pp. R1–R39, Mar. 2007.

[10] R. Akiyama, A. Matsuhisa, J. T. Pearson, and H. Tazawa, "Long-term measurement of heart rate in chicken eggs," *Comp. Biochem. Physiol. Part A Mol. Integr. Physiol.*, vol. 124, no. 4, pp. 483–490, Dec. 1999.

[11] F. Bamelis *et al.*, "Non-destructive Measurements on Eggs During Incubation," *Avian Poult. Biol. Rev.*, vol. 15, pp. 150-159(10), 2004.

[12] A. A. L. J W Bellville, "Method for study of electrocardiogram of early chick embryo within the shell.," *Proc. Soc. Exp. Biol. Med.*, vol. 93, no. 1, pp. 27–30, 1956.

[13] A. Romanoff, *The avian embryo structural and functional development*. New York: Macmillan, 1960.

[14] J. Y. Bogue, "The Heart Rate of the Developing Chick," *J. Exp. Biol.*, vol. 9, no. 4, pp. 351–358, Oct. 1932.

[15] H. Tazawa and G. C. Whittow, "Embryonic heart rate and oxygen pulse in two procellariiform seabirds, Diomedea immutabilis and Puffinus pacificus," *J. Comp. Physiol. B*, vol. 163, no. 8, pp. 642–648, Mar. 1994, doi: 10.1007/BF00369514.

[16] A. E. Aubert, C. Leribaux, F. Beckers, D. Ramaekers, and D. Berckmans, "Noninvasive measurement of heart rate from chicken embryos in the egg," *Comput. Cardiol.*, vol. 27, pp. 227–230, 2000.

[17] W. Burggren and A. Ar, "Continuous measurements of instantaneous heart rate and its fluctuations before and after hatching in chickens," *J. Exp. Biol.*, vol. 203, no. Pt5, pp. 895–903, 2000.

[18] M. . Haque, W. Watanabe, H. Ono, Y. Sakamoto, and H. Tazawa, "Comparisons between invasive and noninvasive determinations of embryonic heart rate in chickens," *Comp. Biochem. Physiol. Part A Physiol.*, vol. 108, no. 2–3, pp. 221–227, Jun. 1994.

[19] J. R. Cain, U. K. Abbott, and V. L. Rogallo, "Heart rate of the developing chick embryo.," *Proc. Soc. Exp. Biol. Med.*, vol. 126, no. 2, pp. 507–10, Nov. 1967.

[20] H. Rahn, S. A. Poturalski, and C. V. Paganelli, "The acoustocardiogram: a noninvasive method for measuring heart rate of avian embryos in ovo," *J. Appl. Physiol.*, vol. 69, no. 4, pp. 1546–1548, Oct. 1990.

[21] N. Wang, J. P. Butler, and R. B. Banzett, "Gas exchange across avian eggshells oscillates in phase with heartbeat," *J. Appl. Physiol.*, vol. 69, no. 4, pp. 1549–1552, Oct. 1990.

[22] A. Youssef, S. Viazzi, V. Exadaktylos, and D. Berckmans, "Non-contact, motion-tolerant measurements of chicken (Gallus gallus) embryo heart rate (HR) using video imaging and signal processing," *Biosyst. Eng.*, vol. 125, pp. 9–16, Sep. 2014.

[23] T. Tamura, Y. Maeda, M. Sekine, and M. Yoshida, "Wearable Photoplethysmographic Sensors—Past and

Present," *Electronics*, vol. 3, no. 2, pp. 282–302, Apr. 2014.

[24] F.-H. Huang, P.-J. Yuan, K.-P. Lin, H.-H. Chang, and C.-L. Tsai, "Analysis of Reflectance Photoplethysmograph Sensors," *Int. J. Biomed. Biol. Eng.*, vol. 5, no. 11, pp. 622–625, Nov. 2011.

[25] Y. Maeda, M. Sekine, T. Tamura, A. Moriya, T. Suzuki, and K. Kameyama, "Comparison of reflected green light and infrared photoplethysmography," in *30th Annual International Conference of the IEEE Engineering in Medicine and Biology Society*, 2008, pp. 2270–2272, doi: 10.1109/IEMBS.2008.4649649.

[26] V. Vizbara, A. Sološenko, D. Stankevičius, and V. Marozas, "Comparison of green, blue and infrared light in wristand forehead photoplethysmography," in *Biomedical Engineering*, 2013, vol. 17, no. 1, pp. 78–81.

[27] S. K. D. Tang, Y. Y. S. Goh, M. L. D. Wong, and Y. L. E. Lew, "PPG signal reconstruction using a combination of discrete wavelet transform and empirical mode decomposition," in *2016 6th International Conference on Intelligent and Advanced Systems (ICIAS)*, 2016, pp. 1–4.

[28] M. Lierz, O. Gooss, and H. M. Hafez, *Noninvasive Heart Rate Measurement Using a Digital Egg Monitor in Chicken and Turkey Embryos*, vol. 20, no. 3. 2006, pp. 141–146.

[29] M. Elgendi, Y. Liang, and R. Ward, "Toward Generating More Diagnostic Features from Photoplethysmogram Waveforms.," *Dis. (Basel, Switzerland)*, vol. 6, no. 1, Mar. 2018.

[30] I. Daubechies, "The wavelet transform, time-frequency localization and signal analysis," *IEEE Trans. Inf. Theory*, vol. 36, no. 5, pp. 961–1005, 1990.

[31] C. Torrence and G. P. Compo, "A Practical Guide to Wavelet Analysis," *Bull. Am. Meteorol. Soc.*, vol. 79, no. 1, pp. 61–78, Jan. 1998.

[32] S. Chopra and K. J. Marfurt, "Choice of mother wavelets in CWT spectral decomposition," in *SEG Technical Program Expanded Abstracts 2015*, 2015, pp. 2957–2961.

[33] D. Komorowski and S. Pietraszek, "The Use of Continuous Wavelet Transform Based on the Fast Fourier Transform in the Analysis of Multi-channel Electrogastrography Recordings," *J. Med. Syst.*, vol. 40, no. 1, p. 10, Jan. 2016.

[34] L. A. Montejo and L. E. Suarez, "An improved CWT-based algorithm for the generation of spectrum-compatible records," *Int. J. Adv. Struct. Eng.*, vol. 5, no. 1, p. 26, Dec. 2013.

[35] L. Li, "A New Method of Wavelet Transform Based on FFT for Signal Processing," in *2010 Second WRI Global Congress on Intelligent Systems*, 2010, pp. 203–206.

[36] J. S. Sahambi, S. N. Tandon, and R. K. P. Bhatt, "Using wavelet transforms for ECG characterization. An on-line digital signal processing system," *IEEE Eng. Med. Biol. Mag.*, vol. 16, no. 1, pp. 77–83, 1997.

[37] N. Zaccarelli, B.-L. Li, I. Petrosillo, and G. Zurlini, "Order and disorder in ecological time-series: Introducing normalized spectral entropy," *Ecol. Indic.*, vol. 28, pp. 22–30, May 2013.

[38] Liang-Sheng Huang and Chung-Ho Yang, "A novel approach to robust speech endpoint detection in car environments," in *2000 IEEE International Conference on Acoustics, Speech, and Signal Processing. Proceedings (Cat. No.00CH37100)*, vol. 3, pp. 1751–1754.

[39] X. Li, H. Liu, Y. Zheng, and B. Xu, "Robust Speech Endpoint Detection Based on Improved Adaptive Band-Partitioning Spectral Entropy," in *Bio-Inspired Computational Intelligence and Applications*, Berlin, Heidelberg: Springer Berlin Heidelberg, 2007, pp. 36–45.

[40] A. VanBrecht, H. Hens, J. Lemaire, J. Aerts, P. Degraeve, and D. Berckmans, "Quantification of the heat exchange of chicken eggs," *Poult. Sci.*, vol. 84, no. 3, pp. 353–361, Mar. 2005.

[41] M. Bressan and T. Mikawa, "Avians as a model system of vascular development.," *Methods Mol. Biol.*, vol. 1214, pp. 225–42, 2015.

[42] L. Pardanaud, D. Luton, M. Prigent, L. Bourcheix, M. Catala, and F. Dieterlen-Lievre, "Two distinct endothelial lineages in ontogeny, one of them related to hemopoiesis," *Development*, vol. 122, no. 5, pp. 1363–1371, 1996.

[43] D. Reese, C. Hall, and T. Mikawa, "Negative Regulation of Midline Vascular Development by the Notochord," *Dev. Cell*, vol. 6, no. 5, 2004.

[44] R. J. Garriock, C. Czeisler, Y. Ishii, A. M. Navetta, and T. Mikawa, "An anteroposterior wave of vascular inhibitor downregulation signals aortae fusion along the embryonic midline axis.," *Development*, vol. 137, no. 21, pp. 3697–706, Nov. 2010.

[45] B. M. Patten and T. C. Kramer, "The initiation of contraction in the embryonic chick heart," *Am. J. Anat.*, vol. 53, no. 3, pp. 349–375, Nov. 1933.

[46] M. T. Politi *et al.*, "The dicrotic notch analyzed by a numerical model," *Comput. Biol. Med.*, vol. 72, pp. 54–64, May 2016.